AIP Journal of Applied Physics

Electromigration in Sn–Cu intermetallic compounds

C. C. Wei, C. F. Chen, P. C. Liu, and Chih Chen

Citation: Journal of Applied Physics **105**, 023715 (2009); doi: 10.1063/1.3072662
View online: http://dx.doi.org/10.1063/1.3072662
View Table of Contents: http://scitation.aip.org/content/aip/journal/jap/105/2?ver=pdfcov
Published by the AIP Publishing

Articles you may be interested in

Influence of Cu column under-bump-metallizations on current crowding and Joule heating effects of electromigration in flip-chip solder joints
J. Appl. Phys. **111**, 043705 (2012); 10.1063/1.3682484

Blocking hillock and whisker growth by intermetallic compound formation in Sn-0.7Cu flip chip solder joints under electromigration
J. Appl. Phys. **107**, 093715 (2010); 10.1063/1.3410796

In situ measurement of electromigration-induced transient stress in Pb-free Sn–Cu solder joints by synchrotron radiation based x-ray polychromatic microdiffraction
J. Appl. Phys. **106**, 023502 (2009); 10.1063/1.3157196

Electromigration induced high fraction of compound formation in SnAgCu flip chip solder joints with copper column
Appl. Phys. Lett. **92**, 262104 (2008); 10.1063/1.2953692

Polarity effect of electromigration on kinetics of intermetallic compound formation in Pb-free solder V-groove samples
J. Appl. Phys. **97**, 063514 (2005); 10.1063/1.1861151

Re-register for Table of Content Alerts

Create a profile.
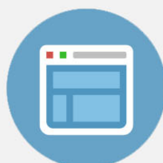
Sign up today!

[This article is copyrighted as indicated in the article. Reuse of AIP content is subject to the terms at: http://scitation.aip.org/termsconditions. Downloaded to] IP: 140.113.38.11 On: Wed, 30 Apr 2014 15:33:20

Electromigration in Sn–Cu intermetallic compounds

C. C. Wei, C. F. Chen, P. C. Liu, and Chih Chen[a)]
Department of Materials Science and Engineering, National Chiao Tung University, Hsin-chu, Taiwan 30010, Republic of China

(Received 15 June 2008; accepted 9 December 2008; published online 30 January 2009)

As the shrinking in bump size continues, the effect of intermetallic compounds (IMCs) on electromigration becomes more pronounced. Electromigration in Sn–Cu intermetallic compounds was examined using edge displacement method. It was found that Cu_6Sn_5 compounds are more susceptible to electromigration than Cu_3Sn compounds. The lower solidus temperature and higher resistivity of the Cu_6Sn_5 IMCs are responsible for its higher electromigration rate. Length-dependent electromigration behavior was found in the stripes of various lengths and the critical length was determined to be between 5 and 10 μm at 225 °C, which corresponded to a critical product between 2.5 and 5 A/cm. Furthermore, the Sn–Cu compounds were proven to have better electromigration resistance than eutectic SnAgCu solder. © *2009 American Institute of Physics*. [DOI: 10.1063/1.3072662]

I. INTRODUCTION

With continuous downward scaling of microelectronic devices, flip-chip technology has become the solution for fine-pitch package in the microelectronics industry.[1] Accompanying the trend of the high performance requirement for central processing units, the size of the solder bumps also decreases. Bumps with nominal diameters of 25 μm have been fabricated.[1] Thus, electromigration has become a critical reliability issue for high performance devices.[2]

During electromigration, the solder may react with the layer of under-bump-metallization (UBM) to form intermetallic compounds (IMCs) and then the passivation opening is depleted. As the dimension of the solder bump decreases, the influence of the IMC layer on electromigration becomes more significant. On the other hand, several approaches have been proposed to prolong the electromigration lifetime of the solder joints.[3–7] Due to the adoption of Pb-free solders, the UBM layer becomes thicker than that in Pb-containing solder because Pb-free solders consume more metallization layer. Nah *et al.* proposed using a thick Cu column as the UBM material and only a small amount of solder is needed. The bump height is as low as 20 μm.[3] During electromigration, extensive Cu–Sn IMCs formed in the joints. In addition, some of the IMC layer may bridge the joints or even the entire solder joints can be transformed into IMC joints. Therefore, the IMC layer may play a key role in electromigration in the solder joints with a low bump height. The Cu–Sn IMCs may have better electromigration resistance than the solder since electromigration voids usually form in the interface of the solder and the IMCs.[8] However, there is no quantitative measurement on the electromigration behavior in the Cu–Sn IMCs.

It is difficult to fabricate IMC joints without solder connecting to them since the IMC is the reaction product between the metallization layer and the solder. Although selective etching method can be used to etch away the solder, the surface morphology of the IMCs is quite rough, making this approach unsuitable for fabricating electromigration pattern of the IMCs. In this study, a unique process is employed to fabricate the Cu–Sn IMCs of Blech structures for electromigration test. Using a focus ion beam (FIB), short IMC stripes of 5, 10, 15, 20, 30, and 40 μm can be fabricated. Electromigration tests were performed in these stripes. Thus, the critical product of the IMCs can be obtained. In addition, an independent electromigration study on eutectic SnAgCu solder stripes was also conducted to measure the critical product of the solder. Thus the electromigration resistance of the IMCs and the solder can be compared directly.

II. EXPERIMENTAL

To examine the critical product of the Sn–Cu IMCs, short Blech stripes of various lengths need to be fabricated. In our previous publication,[9] we reported an approach for preparing solder stripes of various lengths using FIB cutting. Similar approaches were adopted to fabricate the IMC stripes. With the aid of selective etching, the fabrication of the IMC stripes can be realized. Figures 1(a)–1(d) show the schematic drawing of the fabrication processes. By using the lithography technique, patterned 8000 Å Ti/7500 Å Cu metallization layers were fabricated as UBM layers in 10-μm-deep Si trenches, as shown in the cross-sectional schematic in Fig. 1(a). Then the sample was placed under an optical microscope for the placement of Sn0.7Cu solder paste. There were tiny Sn0.7Cu solder balls ranging from 20 to 45 μm in the solder paste. We used a needle to move the solder balls manually to cover the surface of the Ti/Cu metallization layers. The accuracy for placing the solder balls was about 10 μm. Once it was done, the sample was reflowed at 250 °C for 4 s on a hot plate. Figure 1(b) illustrates the cross-sectional schematic after the reflowing process. The Sn–Cu IMCs formed during the reflowing process. Yet, the shape of the Cu_6Sn_5 IMC appears to be scalloplike, which is not suitable for electromigration test. This is be-

[a)]Author to whom correspondence should be addressed. Electronic mail: chih@mail.nctu.edu.tw.

 © 2009 American Institute of Physics

[This article is copyrighted as indicated in the article. Reuse of AIP content is subject to the terms at: http://scitation.aip.org/termsconditions. Downloaded to] IP: 140.113.38.11 On: Wed, 30 Apr 2014 15:33:20

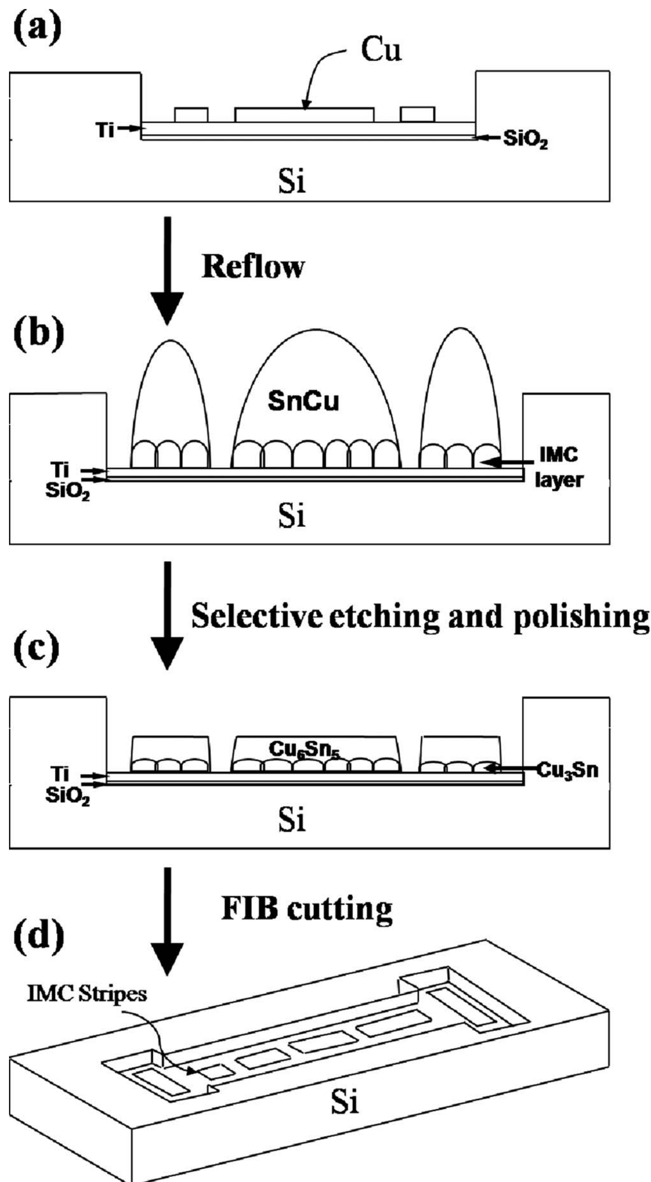

FIG. 1. Schematic drawing for the fabrication processes of the test samples. (a) For the patterned Ti/Cu films in a Si trench. (b) After the reflowing of the SnCu solder on the Ti/Cu UBM. (c) After the selective etching of the solder and the polishing processes. (d) After the FIB etching.

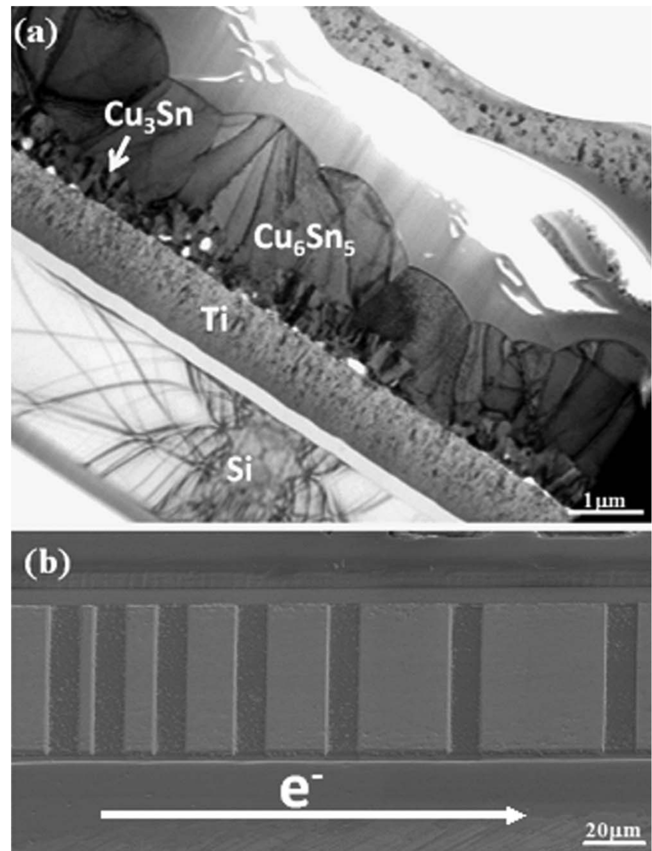

FIG. 2. (a) Cross-sectional TEM image of the test sample after the reflowing and aging process. Both Cu_3Sn and Cu_6Sn_5 layers formed in the sample and the Cu layer was consumed completely. (b) Plan-view SEM image showing the surface morphology after the polish and FIB processes. Various segments including 5, 10, 15, 20, 30, and 40 μm stripes can be prepared.

cause there are gaps among the scalloplike Cu_6Sn_5 IMC, resulting in a nonuniform current distribution in the IMC layer. Thus, a solid-stage aging at 150 °C for 10 h was employed to smooth the Cu_6Sn_5 layer. The purpose of this annealing was to consume the remaining Cu layer into Cu–Sn IMCs. In addition, it also converted the scalloplike Cu_6Sn_5 IMC into a layerlike layer. The selective etching was employed to remove the solder layer by the mixture solution of concentrated nitric acid, acetic acid, and glycerol. A slight polishing was performed to make the surface even smooth, as depicted in Fig. 1(c). Next, FIB was employed to cut a 370-μm-long stripe into desired segments, as shown in Fig. 1(d). After the FIB cutting, the solder may be damaged by the bombardment of Ga ions. Thus, a solid-state aging at 150 °C for 5 h was performed to remove the damage caused by the FIB etching. The thicknesses of the Cu_6Sn_5 and Cu_3Sn layers may not change during this annealing since there was no Cu available for reaction and the annealing time is short.

Figure 2(a) shows the cross-sectional transmission electron microscope (TEM) image of the Blech structure after the liquid-state and solid-state reactions. Both Cu_6Sn_5 and Cu_3Sn IMCs were formed and their thicknesses were 1.36 and 0.37 μm, respectively. The Cu film was consumed completely, which is good for the electromigration study of the IMCs. Otherwise, most of the current might flow in the remaining Cu layer since Cu has much lower resistivity than the IMCs. Figure 2(b) shows the scanning electron microscope (SEM) images for the IMC stripes after the FIB cutting. It can be seen that nice IMC Blech structure can be fabricated using this approach. Stripes of various lengths were prepared, including 5, 10, 15, 20, 30, and 40 μm stripes.

For the IMC electromigration test, the stripes were stressed in a tube oven maintained at 10^{-3} torr vacuum to prevent the IMCs from being oxidized since the test temperature may be as high as 225 °C. For solder electromigration test, the stripes were subjected to a desired current at 150 °C on a hot plate. Figure 3 shows the cross-sectional schematic for the current flows in the stripes. On the basis of the resistivity and thickness of the Ti, Cu_6Sn_5, and Cu_3Sn layers, the resistance ratio of the three layers can be calculated. Then the current flow in each layer is inversely proportional to

[This article is copyrighted as indicated in the article. Reuse of AIP content is subject to the terms at: http://scitation.aip.org/termsconditions. Downloaded to] IP: 140.113.38.11 On: Wed, 30 Apr 2014 15:33:20

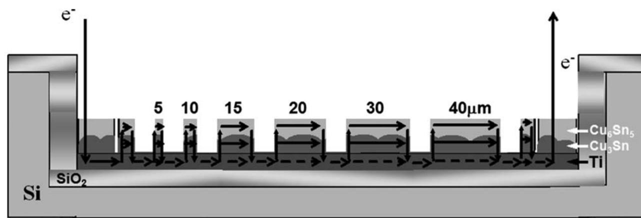

FIG. 3. Schematic showing the electron flow of the test sample.

their resistances. The resistivities for Ti, Cu_3Sn, and Cu_6Sn_5 are 42, 8.3, and 17.5 $\mu\Omega$ cm, respectively.[10] The width for the Ti layer is 100 μm, while it is 78 μm for both IMC layers. The thicknesses for the Ti, Cu_3Sn, and Cu_6Sn_5 layers are 0.8, 0.37, and 1.36 μm, respectively. Therefore, the current percentages in the Ti, Cu_3Sn, and Cu_6Sn_5 layers are 24%, 37%, and 36%, respectively.

Field-emission SEM of JEOL 6500 was employed to observe the surface microstructure, and energy dispersive spectroscopy (EDS) was used to analyze compositions. X-ray mapping in the electron probe microanalyzer (EPMA) (JEOL JXA-8800M) was also used to detect the distribution of Sn and Cu atoms.

III. RESULTS AND DISCUSSION

Length-dependent electromigration behavior was observed in the Sn–Cu IMC stripes and the critical length could be determined. Figure 4(a) shows the SEM image of the Sn–Cu IMC stripes in Fig. 2(b) after the current stressing at 225 °C for 366 h. The thicknesses of the Cu_6Sn_5 and Cu_3Sn layers were 0.65 and 0.37 μm, respectively. The electrons drifted from the left-hand side to the right-hand side. The current densities in the Cu_6Sn_5 and Cu_3Sn layers were 5×10^3 and 9.9×10^3 A/cm^2, respectively. Electromigration-induced voids formed at the cathode ends of the 10-μm-long and longer stripes. In addition, more voids occurred in longer stripes, which suggest that there was back stress in the solder stripes during current stressing. It is worth noting that some smaller voids were formed randomly in the stripes after the current stressing, which may be attributed to the densification of the IMCs at 225 °C for 366 h and they are irrelevant to the electromigration effect. In addition, no voids were found in the 5-μm-long stripes, even when the stripes were stressed up to 900 h, as illustrated in Fig. 4(b). More depletions were observed in longer stripes. Therefore, the critical length of the IMCs was determined to be 5–10 μm and the corresponding critical product was between 2.5 and 5 A/cm at 225 °C.

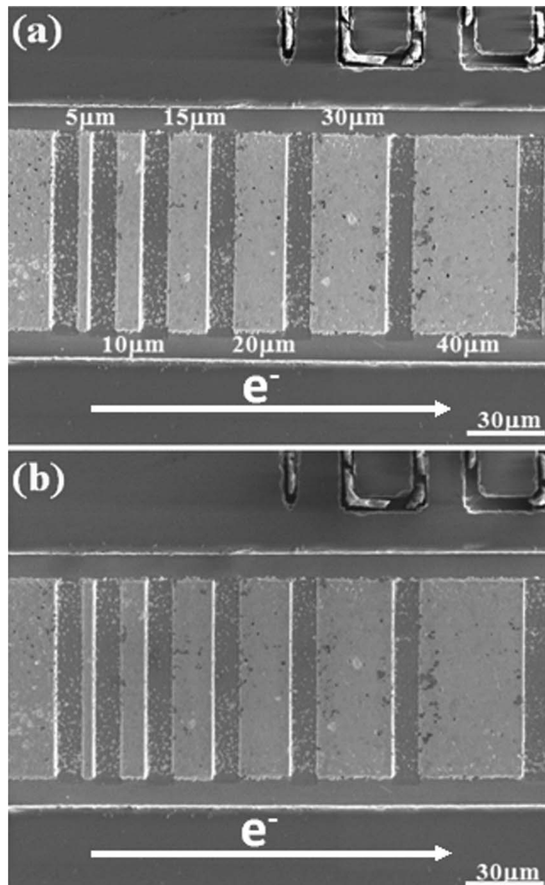

FIG. 4. (a) SEM image showing the Sn–Cu IMC stripes in Fig. 1(b) after the current stressing at 225 °C for 366 h. (b) The same sample in (a) after the current stressing at 225 °C for 900 h. More depletion occurred in longer stripes and no voids were found in the 5 μm stripe.

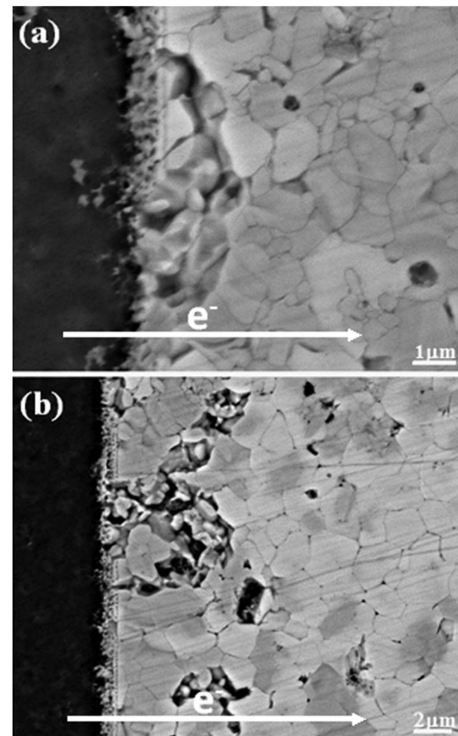

FIG. 5. Enlarged backscattered SEM images for the voids formed in the (a) 10-μm-long stripe and (b) 40-μm-long stripe for the sample shown in Fig. 2(b).

It is interesting to note that the Cu_6Sn_5 layer was depleted before the Cu_3Sn layer, even though the current density in the Cu_3Sn layer was higher. Figures 5(a) and 5(b) show the enlarged SEM image for the electromigration-induced voids formed in the cathode ends of the 10-μm-long and 40-μm-long stripes. It seems that the Cu_3Sn layer remained on the Ti layer after the depletion of the Cu_6Sn_5 layer. To detect the surface composition more accurately, SEM EDS operated at 5 kV was employed to analyze the composition on the surface of the stripes. It is found that the

[This article is copyrighted as indicated in the article. Reuse of AIP content is subject to the terms at: http://scitation.aip.org/termsconditions. Downloaded to] IP: 140.113.38.11 On: Wed, 30 Apr 2014 15:33:20

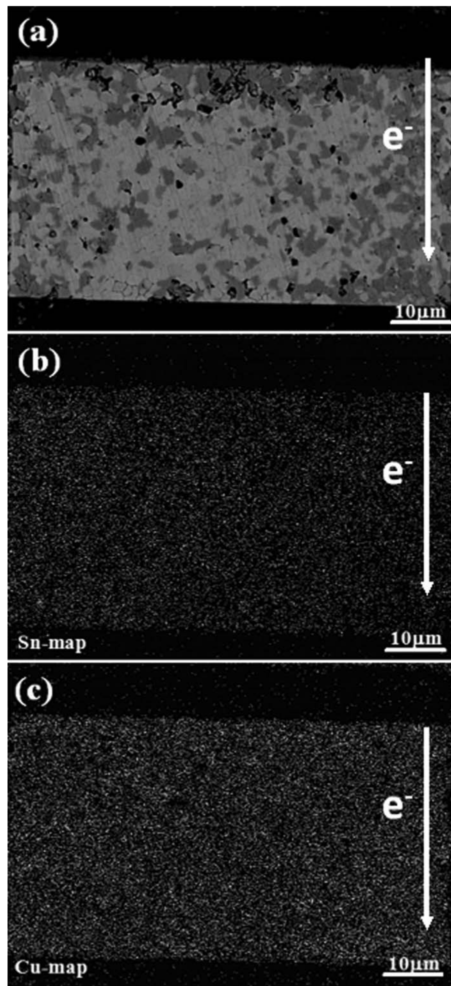

FIG. 6. (a) Backscattered SEM image of the 40-μm-wide stripes for the sample shown in Fig. 2(b). (b) The corresponding x-ray mapping of Sn atoms. (c) The corresponding x-ray mapping of Cu atoms.

composition in the depleted region was very close to 75 at. % Cu and 25 at. % Sn, which is the composition of Cu_3Sn. On the other hand, the composition in the undepleted regions was about 58 at. % Cu and 42 at. % Sn, which is close to the composition of Cu_6Sn_5. Thus, it is speculated that Cu_6Sn_5 is more susceptible to electromigration than Cu_3Sn. This may be mainly attributed to the following reasons. The solidus temperature for Cu_6Sn_5 is 415 °C, whereas it is 676 °C for Cu_3Sn.[11] Therefore, the diffusion rate for Cu_6Sn_5 at the electromigration temperature is higher. Also, Cu_6Sn_5 could diffuse through the free surface, whereas it is not possible for Cu_3Sn because it is sandwiched between Cu_6Sn_5 and the Ti layers, as shown in Fig. 2(a). Furthermore, the critical length, L_c, can thus be expressed as[2]

$$L_c = \frac{\sigma_c \Omega}{Z^* e j \rho}, \quad (1)$$

where σ_c is the stress at the critical length, e is the charge of electron, j is the applied current density, ρ is the resistivity, Ω is the atomic volume, and Z^* is the effective charge number. The critical length is inversely proportional to the resistivity. The resistivities for the Cu_6Sn_5 and Cu_3Sn IMCs are 17.5 and 8.3 $\mu\Omega$ cm, respectively. The resistivity difference

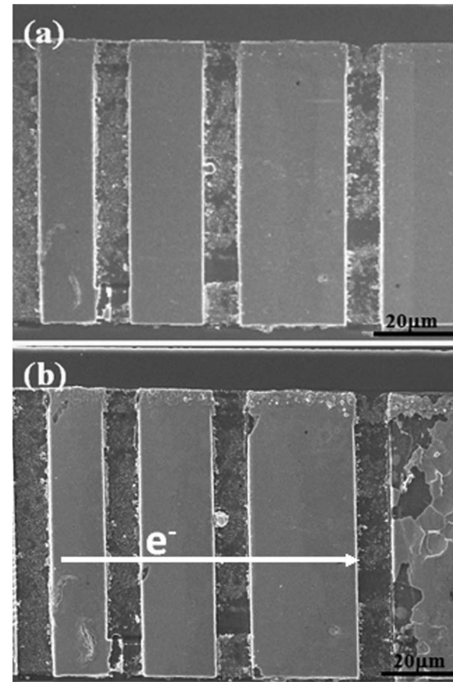

FIG. 7. Secondary SEM images for the eutectic SnAgCu solder stripes (a) before and (b) after the stressing by 2×10^4 A/cm^2 at 225 °C for 330 h. Serious depletion occurred in the 40-μm-long SnAgCu stripe.

also supports Cu_6Sn_5 being more easily migrated by electrons. Therefore, the measured critical product is for the Cu_6Sn_5 IMCs. However, the effective charge numbers for the Cu_6Sn_5 and Cu_3Sn compounds have not been measured yet and it deserves further study.

To examine which atoms serve the dominant diffusion species, x-ray mapping in the EPMA was performed on all the stripes in Fig. 4(b). Figure 6(a) shows the backscattered SEM image for the 40-μm-wide stripes after the stressing at 225 °C for 900 h. The corresponding mapping of Sn and Cu atoms is depicted in Figs. 6(b) and 6(c), respectively. No obvious depletion or buildup of Sn or Cu atoms was found after the electromigration test. In addition, SEM EDS analysis suggests no detectable composition fluctuation of Sn or Cu atoms in the middle and the anode end of the stripes. Therefore, the dominant diffusion species is not clear at this moment.

To compare the electromigration resistance of the Cu_6Sn_5 IMCs to the solder, another electromigration experiment was performed on the eutectic SnAgCu solder stripes with the same pattern. Wei *et al.* performed electromigration in eutectic SnPb solder stripes and the critical product is determined to be between 20 and 30 A/cm at 100 °C. In this study, the critical product for the IMC was measured to be between 2.5 and 5 A/cm at 225 °C. Because of the temperature difference, these two values cannot be compared directly. In addition, it is reported that Pb-free solders have better electromigration resistance than the eutectic SnPb solder.[12] Thus, to obtain a direct comparison, stripes of the eutectic SnAgCu solder and the IMCs were stressed at the same condition at a lower temperature of 150 °C. Figures 7(a) and 7(b) present the SEM images for the solder before and after the stressing at 2×10^4 A/cm^2 at 150 °C for 330

[This article is copyrighted as indicated in the article. Reuse of AIP content is subject to the terms at: http://scitation.aip.org/termsconditions. Downloaded to] IP: 140.113.38.11 On: Wed, 30 Apr 2014 15:33:20

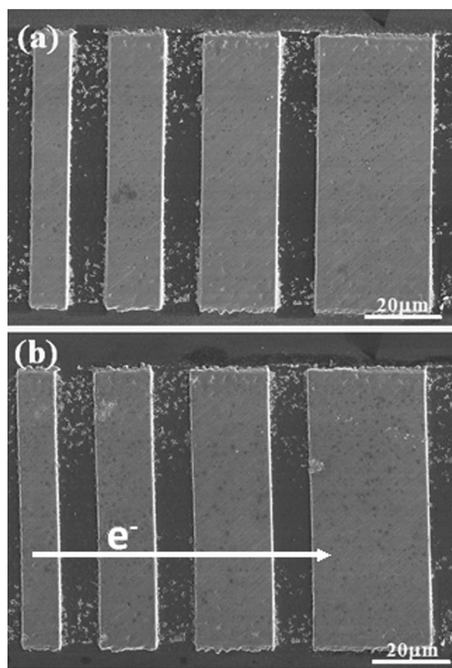

FIG. 8. Secondary SEM images for the IMC solder stripes (a) before and (b) after the stressing by 2×10^4 A/cm^2 at 225 °C for 330 h. No depletion occurred in all the IMC stripes.

h. It is found that clear voids occurred in the SnAgCu stripes. Serious depletion occurs at the cathode end of the stripe on the far right-hand side. Small voids formed on the 20 and 30 μm stripes. On the other hand, Figs. 8(a) and 8(b) present the SEM images for the IMCs before and after the stressing at 2×10^4 A/cm^2 at 150 °C for 330 h. All the IMC stripes stay intact after the current stressing. Therefore, it is confirmed that the IMCs have better electromigration resistance than the eutectic SnPb and SnAgCu solders.

IV. CONCLUSIONS

The electromigration behavior has been examined using short Blech stripes fabricated by lithography and FIB etching. It is found that the Cu_6Sn_5 IMCs have a much higher electromigration rate than the Cu_3Sn IMCs. Both Cu and Sn atoms move during the electromigration test. The lower solidus temperature and higher resistivity of the Cu_6Sn_5 IMCs are responsible for its higher electromigration rate. By applying the current stressing at 5×10^3 A/cm^2 at 225 °C for 900 h, the critical length of the Cu_6Sn_5 IMCs was determined to be between 5 and 10 μm. The corresponding critical product was between 2.5 and 5 A/cm at 225 °C. An independent experiment was also performed to verify that the electromigration resistance of the IMCs was superior to the eutectic SnAgCu solder.

ACKNOWLEDGMENTS

The authors would like to thank the National Science Council of Republic of China for financial support through Grant No. 95-2221-E-009-088MY3.

[1] S. L. Wright, R. Polastre, H. Gan, L. P. Buchwalter, R. Horton, P. S. Andry, E. Sprogis, C. Patel, C. Tsang, J. Knickerbocker, J. R. Lloyd, A. Sharma, and M. S. Sri-Jayantha, *Proceedings of the 56th Electronic Components and Technology Conference* (IEEE Components, Packaging, and Manufacturing Technology Society, San Diego, CA, 2006), p. 633.
[2] K. N. Tu, J. Appl. Phys. **94**, 5451 (2003).
[3] J. W. Nah, J. O. Suh, K. N. Tu, S. W. Yoon, V. S. Rao, V. Kripesh, and F. Hua, J. Appl. Phys., **100**, 123513 (2006).
[4] S. W. Liang, Y. W. Chang, and C. Chen, Appl. Phys. Lett. **88**, 172108 (2006).
[5] S. W. Liang, T. L. Shao, C. Chen, E. C. C. Yeh, and K. N. Tu, J. Mater. Res. **21**, 137 (2006).
[6] C. Chen and S. W. Liang, J. Mater. Sci.: Mater. Electron. **18**, 259 (2006).
[7] S. W. Liang, Y. W. Chang, and C. Chen, J. Electron. Mater. **36**(2), 159 (2007).
[8] L. Zhang, S. Ou, J. Huang, K. N. Tu, S. Gee, and L. Nguyen, Appl. Phys. Lett. **88**, 012106 (2006).
[9] C. C. Wei and C. Chen, Appl. Phys. Lett. **88**, 182105(2006).
[10] *The Mechanics of Solder Alloy Interconnects*, edited by D. R. Frear, S. N. Burchett, H. S. Morgan, and J. H. Lau (Van Nostrand Reinhold, New York, 1994), p. 60.
[11] N. Saunders and A. P. Miodownik, Bull. Alloy Phase Diagrams **11**, 278 (1990).
[12] Y. S. Lai, K. M. Chen, C. L. Kao, C. W. Lee, and Y. T. Chiu, Microelectron. Reliab. **47**, 1273 (2007).

[This article is copyrighted as indicated in the article. Reuse of AIP content is subject to the terms at: http://scitation.aip.org/termsconditions. Downloaded to] IP: 140.113.38.11 On: Wed, 30 Apr 2014 15:33:20